FLOMEKO2019
18th International Flow Measurement Conference
Portugal | Lisbon | LNEC | 26-28 june 2019

Design of a Calibration System for Miniature Carbon Dioxide Sensors

Mengna Li[1], Heming Hu[1], Jing Zhang[1]

1Division of Thermophysics and Process Measurements, National Institute of Metrology, No.18 Bei San Huan Dong Lu, Chaoyang District, Beijing 100013, China
E-mail (corresponding author): limn@ nim.ac.cn

Abstract

Anthropogenic activities such as combustion of fossil fuel and changes in land use release carbon dioxide (CO_2) into the atmosphere which impacts climate. Cities, with high energy consumption, are main emitters of CO_2.Therefore, acquiring the concentration and movement of CO_2 in cities is the key to the mitigation of CO_2 emission and the implementation of policies designed for climate change adaption. To quantify the CO_2 emission from cities and investigate its contribution to the regional carbon budget, it is necessary to employ a multi-point observation method. The miniature non-dispersive infrared (NDIR) sensor, which is inexpensive, stable and can provide with high spatial and temporal resolution data, is preferable. However, the emission status of CO_2 can not be well researched without high-quality observed data. It is important to correct the sensors' outputs to enhance the accuracy. Focusing on this, we develop a calibration system of the NDIR CO_2 sensors (Senseair K30). A theoretical transmission model is established based on the Beer-Lambert law. Observed signals of K30 sensor and high-precision Picarro CO_2 analyzer are recorded, along with temperature and pressure obtained by BME sensor, and then theoretical transmission using the experimentally observed variations is calculated. Finally, the theoretical transmission is fitted to the experimental data using a polynomial function, and a reasonable correction formula is established. In this study, we explore the measurement principle of NDIR sensors and develope a feasible methodology for the calibration of miniature CO_2 sensors. This paper provides a reference for improving the accuracy of miniature CO_2 sensors, which is essential for a comprehensive understanding of the CO_2 emission status.

1. Introduction

Anthropogenic activities such as combustion of fossil fuel and changes in land use release carbon dioxide (CO_2) into the atmosphere which impacts climate [1, 2]. Cities, with high energy consumption, are main emitters of CO_2. Therefore, acquiring the concentration and movement of CO_2 in cities is the key to the mitigation of CO_2 emission and implementation of policies designed for climate change adaption.

Quantifying the CO_2 emission from cities and investigating its contribution to the regional carbon budget, it is necessary to employ a multi-point observation method using as many fixed stations or observation vehicles as possible [3]. For multi-point observation, low-cost but accurate sensors are preferable. The miniature non-dispersive infrared (NDIR) sensors, which are inexpensive, stable and can provide with high spatial and temporal resolution data, are widely in high-density CO_2 observation network.

Performance of miniature NDIR sensors can significantly impact the accuracy of the CO_2 emission measurement. The output of sensors is affected by many facotrs such as temperature, atmospheric pressure, and length of use [4-6]. Without high-quality data, the emission status of CO_2 can not be well researched. To enhance the accuracy of miniature NDIR sensors, it is important to correct the sensors' outputs. Therefore, a calibration method to improve the precision and accuracy of recently developed miniature CO_2 sensors is required. However, few studies focused on the performance and calibration methods of small commercial CO_2 sensors [7, 8].

The objectives of this study are to explore the principle of NDIR sensor and develope a feasible methodology for the calibration of miniature CO_2 sensors. Focusing on this, we develop a calibration system of the NDIR CO_2 sensors (Senseair K30) to improve the accuracy of the measurement. In this study, theoretical data based on the experimental variables is calculated. The observed data

is recorded and compared with the data measured by a highly accurate CO_2 analyzer (Piccrao-G2401). Using analytical methodology, the theoretical data is fitted to the observed data, and a reasonable correction formula is established. This paper provides a reference for the calibration system of improving the accuracy of miniature CO_2 sensors, which is essential for a comprehensive understanding of the CO_2 emission status.

2. The miniature CO_2 sensor

2.1 Senseair K30 overview

The Senseair K30 non-dispersive infrared (NDIR) CO_2 sensor, which is shown in Figure 1, is used commercially for monitoring CO_2 concentration. The measurement range is 0 to 5000 ppm, with an accuracy of ± 3%. The rate of meaurement is 0.5Hz. It is small, lightweight and the dimensions are 51 x 57 x 14 mm (Lengh x Width x approximate Height).

Figure 1: A Senseair K30 NDIR CO_2 sensor

2.2 Measurement principle

The Beer-Lambert law relates the intensity I of radiation, after passage through a length L of a species with concentration c and absorption cross-section σ, to its initial intensity I_0:

$$I = I_0 \, e^{-c\sigma L} \qquad (1)$$

The NDIR sensor measures the intensity signal I of infrared signal after passing through the sample gas. The average transmittance τ is calculated, and the relationship between transmittance and the ratio of sample gas to be measured is established.

The equation can also be expressed as transmission $\tau = I / I_0$; τ is the fraction of incoming radiation that passes through the sample.

$$\tau = \exp(-\sigma(T, P, \upsilon)cL) \qquad (2)$$

The equation can be converted to the relationship with mixing ratio, temperature and pressure.

$$\tau = \exp\left(-\sigma(T, P, \upsilon)\frac{PXN_A}{RT}L\right) \qquad (3)$$

where X is the mixing ratio of the gas to be measured, T the temperature of the air chamber and P is the pressure. N_A is Avogadro constant, and R is the ideal gas constant.

The absorption cross-section σ (T, P,υ), which is the function of temperature and pressure, can be further expressed as the convolution form of the spectral line strength Si and linear function φi of each spectral line in the wavelengh range, and the integral is within the wavelengh range of the sensor spectral band filter. The equation can be expressed as follows,

$$\tau = \frac{1}{\Delta\upsilon}\exp\left(-\sum_i S_i(T)\varphi_i(T, P, \upsilon)\frac{PXN_A}{RT}L\right)\mathrm{d}\upsilon \qquad (4)$$

CO_2 absorbs strongly in the thermal infrared (IR) centred around 2348 cm^{-1}, or 4.26 μm. The relatively high intensity of the peaks in this band makes this wavelength range the most appropriate for a CO_2 sensor [9]. Hence, the spectral band pass filter included in the sensors allows transmission between 2280 and 2400 cm^{-1}. The pass band coincides with a frequency range over which CO_2 absorbs strongly, but H_2O absorbs weak.

3. Methods

3.1 Apparatus

Apparatuses include BME 680 sesnors, Piccrao-G2401 CO_2 concentration analyzer, pump, thermostat, external vents and drying chamber. Connections between different apparatus are shown in Figure 2.

BME680 sensor was used to measure the pressure and temperature in the thermostat during the experiment. The BME680 is a digital 4-in-1 sensor with gas, humidity, pressure and temperature measurement based on proven sensing principles. In addtion, highly accurate Piccrao-G2401 CO_2 concentration analyzer was used for comparison.The analyzer provides simultaneous and continuous measurement of gas. It has a high precision and accuracy, with a parts-per-billion sensitivity. The experimental apparatus is shown in Figure 3.

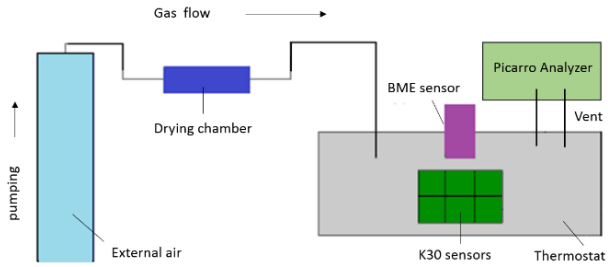

Figure 2: Connections between the apparatus

Figure 3: The experimental apparatus

3.2 Analytical methodology overview

Analytical methodology is used to explore the relationship between the observed data and theoretical data.The process of experiment and data analysis is as follows; Section 3.4 to Section 3.6 provide more detailed information on these steps.

Firstly, a theoretical transmission model as a fuction of temperature, pressure and CO_2 concentration is established based on the Beer-Lambert law. Secondly, the observed signal obtained by K30 and Picarro is recorded, along with temperature and pressure by BME sensor.Thirdly, theoretical transmission based on the experimentally observed variations is calculated using the transmission model. In addtion, to compare the experimentally measured data and theoretical data, the theoretical transmission is fitted to the experimental data using a polynomial function. Finally, a reasonable correction formula is established for the calibration of miniature CO_2 sensors.

3.3 Transmission calculation model

3.3.1 The spectral line strength

The spectral line strength S of CO_2 can be calculated using the following equation:

$$S = S(T_s)\frac{Q_V(T_s)Q_r(T_s)}{Q_V(T)Q_r(T)} exp\left[\frac{1.439E''(T-T_s)}{TT_s}\right] \quad (5)$$

where $S(T_s)$ is the the spectral line strength under standard temperature, E'' is the low-state energy of the transition. Q_V is vibration distribution function, and Q_r is rotation distribution function. Both of them are the function of temperature. Within the temperature range of the 175 ~ 325K, Q_V of CO_2 can be expressed in the following formula [10]:

$$Q_V(T) = 1.05385 - 8.11142 \times 10^{-4}T + 3.18772 \times 10^{-6}T^2 \quad (6)$$

And Q_r can be expressed as:

$$Q_r(T) = Q_r(T_s)\left(\frac{T}{T_s}\right) \quad (7)$$

The CO_2 spectral data used in the calculation is taken from the HITRAN 2016 spectroscopic database [11].

3.3.2 The linear function

The linear function reflects the variation of absorption cross-section with frequency, that is, the line broadening. A transition between two given quantum mechanical energy levels of a molecule occurs at a single, well-defined frequency. Theoretically, a spectroscopic line at this exact frequency should be observed. However, experimentally observed lines have a finite width. This is due to line broadening effects, which cause small differences in transition frequency from the quantum mechanical result. This gives rise to probability distributions around the central line frequency, and a non-zero line width [12].

For gas, the main type of the line broadening are the Doppler non-uniform broadening (Gauss line shape) caused by molecular thermal motion, and uniform broadening (Lorenz line shape) caused by the collision. Pressure broadening is due to collisions between molecules, which lead to some variation in the energies of the rotational and vibrational states of the absorbing species [13]. The line shape in this study is dictated by pressure broadening. Pressure broadening depends not only on pressure, but also the collision between the molecules.There are contributions from the absorbing species and other species in the gas mixture, and the combined effects can be approximated by a Lorentz probability distribution. The Lorentz line shapes:

$$\varphi(T,P,\upsilon) = \frac{\alpha_L}{\pi[(\upsilon-\upsilon_0)^2+\alpha_L^2]} \quad (8)$$

where α_L is the half-width of Lorentz broadening, and can be calculated using

$$\alpha_L(P,T) = \gamma\left(\frac{P}{P_s}\right)\left(\frac{T}{T_s}\right)^{-n} \quad (9)$$

where υ_0 is the centre frequency, γ is the spectral line half-width at standard pressure P_s (1 atmospheric pressure) and standard temperature T_s (296K), n is the temperature coefficient. The value of γ and n are taken from the HITRAN 2016 spectroscopic database.

3.3.3 Integration of the IR absorption spectrum

The calculation of absorption cross-section is based on integration of the IR absorption spectrum. For actual atmospheric molecular spectra, a spectral interval often contains a number of spectral lines. Hence the contributions of all spectral lines should be taken into account when calculating the absorption coefficient at a specific sampling point. Line-by-line integration was adopted in the study.

For all spectral lines, weighted average half-width is used instead.

$$\overline{\alpha_L} = (\sum_{i=1}^{n} \sqrt{S_i \alpha_{Li}} \,/\, \sum_{i=1}^{n} \sqrt{S_i})^2 \qquad (10)$$

In addtion, spectral line center which is not exactly at the integral sampling point was moved to the sampling point. The strength of all spectral lines at the same integral point is summed up and then treated as a single line [14, 15]. In order to compensate the error caused by truncation, the line strength can be modified as follows,

$$S' = S/(1 - \frac{2}{\beta\pi}) \qquad (11)$$

According to the measurement principle of NDIR sensors, the transmission τ of a fixed mixing ratio of CO_2, can be calculated using the Beer-Lambert law. The calculation model is established and then tested using variables (*P* and *T*) that were similar to those in the experiment environment. The value of temperature *T* was set between 273 K and 323 K, and pressure *P* between 0.96 atm and 1.08 atm. The transmission surface is shown in Figure 4.

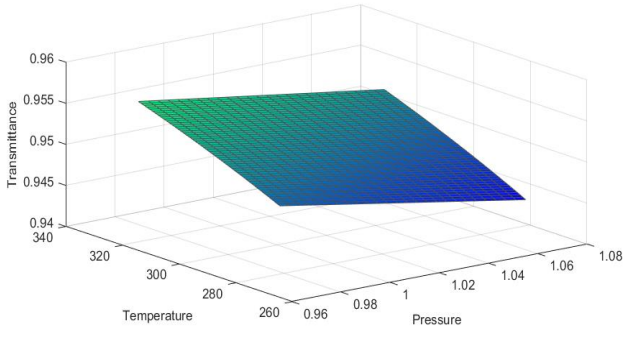

Figure 4: Transmission surfaces

3.4 Experimentally observed data

Experiments were successfully performed over timescale from 16:30 (25 September 2018) to 15:00 (26 September 2018). During the experiment, K30 sensor and BME sensor were placed in the thermostatic box. In series of experiments, external air was pumped through the drying chamber from the atmosphere, and then into the thermostat. In the process of measurement, the inlet of the external air was closed. Picarro analyzer, which has been calibrated using standard gas, was connected to the thermostat through the inlet and outlet vents to provide measurement of the CO_2 concentration.

Continuous observed time-series data during the experiment was recorded. The variation of pressure and temperature were recorded by BME sensor. The CO_2 concentration was measured by K30 sensor and a high-precision Picarro CO_2 analyzer throughout the experiment. Raw signal of K30 sensor is also obtained, which is used to investigate and analyze the correction method of the sensor. The recorded temperature and pressure of BME sensor, and the observed signal of K30 sensor and Picarro analyzer are shown in Figure 5.

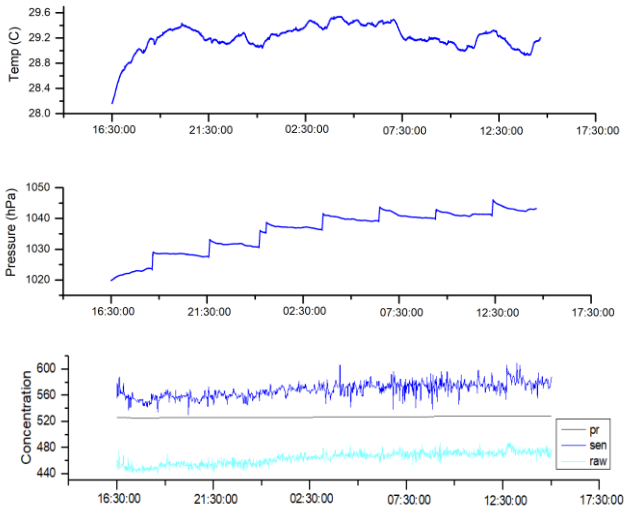

Figure 5: Temperature, pressure recorded by BME sensor; the observed signal by K30 sensors and Picarro analyzer. Line pr represents the data observed by Picarro. Line sen and raw is the observed signal and raw signal of K30, respectively.

3.5 Transmission calculation

Theoretically transmission, based on the variations obtained in the experiment, described in Section 3.4, can therefore be calculated.

The experimental pressure *P* and temperature T are recorded by BME sensor, and *C* is acquired during the experiment using the Picarro analyzer. Initially, using the observed pressure and temperature for the experiment, theoretical transmission is calculated at the CO_2 mixing ratio measured in the experiment. Then the curves of transmisson, as a function of pressure and temperature are plotted in Figure 6. This provides a measure of theoretical transmission to distinguish small changes at different pressures and temperature.

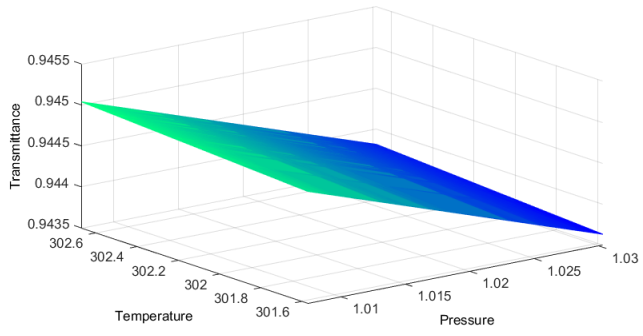

Figure 6: Theoretical transmission surfaces

3.6 Fitting transmission to observed signal

Theoretical transmission can be calculated for a given temperature, pressure and concentration. Correlation analysis is carried out to explore and analyze the relationship between theoretical transmission and the raw signal of K30.

In addtion, experimentally observed signal of K30, based on the analytical methodology, is fitted with exponential function to the theoretically derived transmission. The fitting function is of the cubic form $ax^3 + bx^2 + cx + d$ for an observed signal, where a, b, c and d are constants. Adding a further term has very little effect on the fit.

Regression analysis was used to clarify the relationship between the raw signal of K30 sensor and the output of Picarro analyzer. Accordingly, the correction formula is obtained.

4. Result and Discussion

4.1 Variables dependence

Temperature shows small and rapid changes coincide with the changes during the experiment. Experiments were performed over a timescale of several hours with a sealed apparatus, changes of temperature are due to the change external environment. Pressure profile of the experiment has a typical stepwise variation during the experimental procedure. Pressure increases due to the increase of water vapor in the themostat. The effect of water vapour on the observed signal suggests that absorption is significant at high water vapour mixing ratios over the spectral range of the sensors.

The curves of tansmssion as a function of temperature and pressure are not linear because the concentration is sufficient to make the CO_2 effectively opaque in this spectral region at higher pressures. For large values of *C*, the Beer-Lambert exponent becomes very large and negative.

4.2 Statistical analysis

Using Correlation analysis, the goodness-of-fit between theoretical transmission and raw signal is analyzed. The coefficient of determination (R^2) is 0.9812, indicating a high correlation between theoretical transmission and raw signal. The result is shown in Figure 7, where trans is the theoretical transmission, and raw is the value of raw signal.

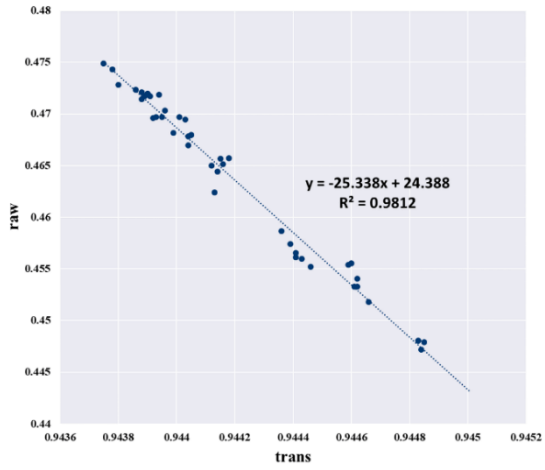

Figure 7: Relationship between theoretical data and the raw signal

The relationship of the sensor output and theoretical calculated transmission is analyzed. The result is shown in Figure 8, which indicates that there is a convertion from the transmission to concertration, and the original signal is corrected using a non-linear function in K30 sensor.

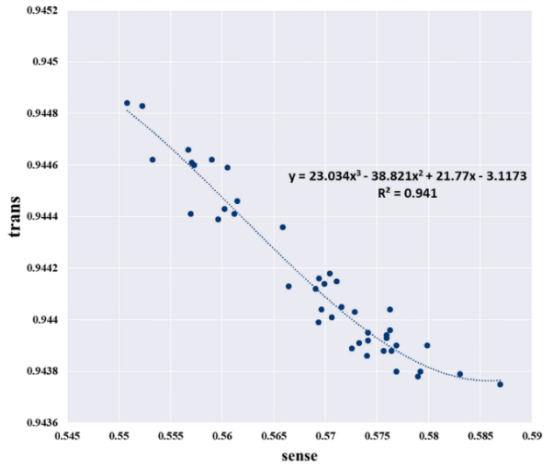

Figure 8: Theoretical data with observed signal of K30

Using Regression analysis, the raw signal of K30 sensors can be fitted to the concentration measured by Picarro analyzer, the result is shown in Figure 9.

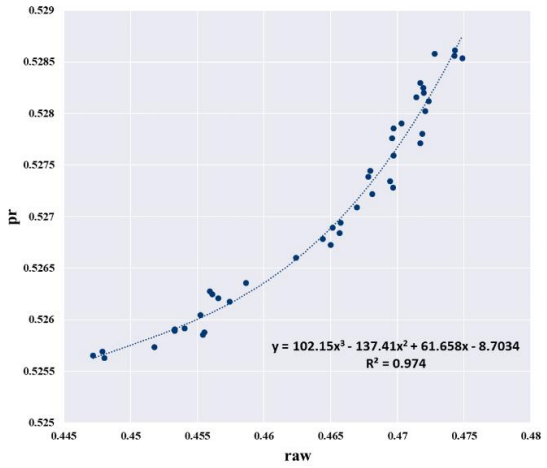

Figure 9: Measurement of Picarro with raw signal of K30

4.3 Validation test

The CO_2 concentration was measured by a high-precision Picarro CO_2 analyzer and K30 sensor using the apparatus described in Section 3.1. The raw signal of the K30 sensor was corrected based on the regression function, and then compared to the measured CO_2 concentration data obtained by the Picarro analyzer. The result is shown in Figure 10.

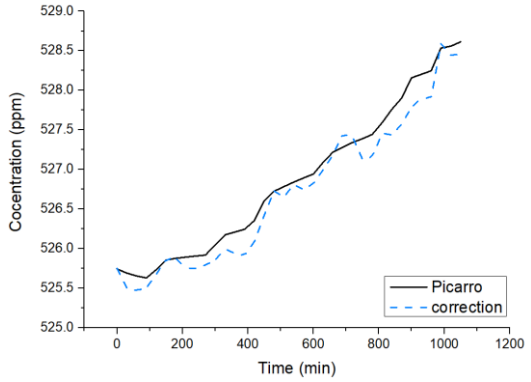

Figure 10: Comparison of CO_2 concentration measured by Picarro and corrected result of K30

Subsequently, the relative root mean squared error (RRMS) difference of the corrected value against the measurement of Picarro analyzer was calculated. The RRMS difference is 0.46%, indicating a good agreement between the corrected value of K30 sensor and the measurement of high-precision Picarro CO_2 analyzer.

5. Conclusion

The principle of minature NDIR sensors is explored and a theoretical transmission model as a fuction of temperature, pressure and CO_2 concentration is established based on the Beer-Lambert law.

In addtion, the experimentally observed signal of senors, along with temperature and pressure are obtained. Using analytical methodology, the theoretical data is calculated and fitted with the observed data. Accordingly, a calibration method of miniature NDIR CO_2 sensors (Senseair K30) to improve the accuracy of the measurement is developed. This study provides a reference for improving the accuracy of miniature CO_2 sensors, which is essential for quantifying and understanding the CO_2 emission status.

There was insufficient time to calculate a theoretical data affected by H_2O absorption, mainly due to a lack of data of fixed H_2O. To quantify the interferent effect of H_2O, further experiment can be conducted to perform the calculation, and fit the signal to sets of data at a series of fixed H_2O values.

Acknowledgments
This paper is currently supported by The National Key R&D Program of China (project/subject SN. 2017YFB0504003)

References

[1] IPCC, Contribution of Working Group I to the Fourth Assessment Report of the Intergovernmental Panel on Climate Change, *The Physical Science Basis*, p. 996, 2007.

[2] Hofmann, D.J., et al., The role of carbon dioxide in climate forcing from 1979 to 2004: introduction of the Annual Greenhouse Gas Index, *Tellus B: Chemical and Physical Meteorology*, **58(5)**, p. 614-619, 2006.

[3] Idso, C.D., S.B. Idso, and R.C. Balling Jr, The urban CO_2 dome of Phoenix, Arizona. *Physical Geograph*, **19(2)**, p.95-108,1998.

[4] Hodgkinson, J., et al., Non-dispersive infra-red (NDIR) measurement of carbon dioxide at 4.2 µm in a compact and optically efficient sensor, *Sensors and Actuators B: Chemical*, **186**, p. 580-588, 2013.

[5] Wong, J.Y., Self-calibration of an NDIR gas sensor, *Google Patents*, 1994.

[6] Mizoguchi, Y. and Y. Ohtani, Comparison of response characteristics of small CO_2 sensors and an improved method based on the sensor response, *Journal of Agricultural Meteorology (Japan)*, 2005.

[7] Grimmond, C., et al., Local-scale fluxes of carbon dioxide in urban environments: methodological challenges and results from Chicago, *Environmental Pollution*, **116**,p. S243-S254, 2002.

[8] Pandey, S.and K.-H.Kim,The relative performance of NDIR-based sensors in the near

real-time analysis of CO_2 in air, *Sensors*, **7(9)**, p. 1683-1696, 2007.

[9] Johns, J., Absolute intensity and pressure broadening measurements of CO_2 in the 4.3-µm region, *Journal of Molecular Spectroscopy*, **125(2)**, p. 442-464, 1987.

[10] McClatchey, R.A., et al., AFCRL atmospheric absorption line parameters compilation, *Air Force Cambridge Research Labs HANSCOM AFB MA*, 1973,

[11] Gordon, I.E., et al., The HITRAN 2016 molecular spectroscopic database, *Journal of Quantitative Spectroscopy and Radiative Transfer*, **203**, p. 3-69, 2017.

[12] Ward, J., J. Cooper, and E.W. Smith, Correlation effects in the theory of combined Doppler and pressure broadening—I. Classical theory, *Journal of Quantitative Spectroscopy and Radiative Transfer*, **14(7)**, p. 555-590, 1974.

[13] Hollas, J.M., *Modern spectroscopy (*John Wiley & Sons), 2004

[14] Aoki, T., An accurate representation of the transmission functions of the H_2O and CO_2 infrared bands, *Journal of Quantitative Spectroscopy and Radiative Transfer*, **24(3)**, p. 191-202, 1980.

[15] Hurst, S., A. Durant, and R. Jones, A low cost, disposable instrument for vertical profile measurements of atmospheric CO_2, *Chemistry Research Project Report*, 2011.